Bone Morphogenetic Protein-2-Induced Signaling and Osteogenesis Is Regulated by Cell Shape, RhoA/ROCK, and Cytoskeletal Tension

Yang-Kao Wang,*,† Xiang Yu,† Daniel M. Cohen, Michele A. Wozniak, Michael T. Yang,
Lin Gao, Jeroen Eyckmans, and Christopher S. Chen

Abstract

Osteogenic differentiation of human mesenchymal stem cells (hMSCs) is classically thought to be mediated by different cytokines such as the bone morphogenetic proteins (BMPs). Here, we report that cell adhesion to extracellular matrix (ECM), and its effects on cell shape and cytoskeletal mechanics, regulates BMP-induced signaling and osteogenic differentiation of hMSCs. Using micropatterned substrates to progressively restrict cell spreading and flattening against ECM, we demonstrated that BMP-induced osteogenesis is progressively antagonized with decreased cell spreading. BMP triggered rapid and sustained RhoA/Rho-associated protein kinase (ROCK) activity and contractile tension only in spread cells, and this signaling was required for BMP-induced osteogenesis. Exploring the molecular basis for this effect, we found that restricting cell spreading, reducing ROCK signaling, or inhibiting cytoskeletal tension prevented BMP-induced SMA/mothers against decapentaplegic (SMAD)1 c-terminal phosphorylation, SMAD1 dimerization with SMAD4, and SMAD1 translocation into the nucleus. Together, these findings demonstrate the direct involvement of cell spreading and RhoA/ROCK-mediated cytoskeletal tension generation in BMP-induced signaling and early stages of in vitro osteogenesis, and highlight the essential interplay between biochemical and mechanical cues in stem cell differentiation.

Introduction

Human mesenchymal stem cells (hMSCs) are multi-potent cells that can differentiate into osteoblasts, chondrocytes, adipocytes, and other connective tissue cells thought to be important in the repair and maintenance of many musculoskeletal tissues [1–4]. The commitment and differentiation of hMSCs to specific lineages appear to be dictated both in vivo and in vitro by their exposure to local cues within their surrounding microenvironment. Osteogenic lineage differentiation of the hMSCs is perhaps the most well described, and the bone morphogenetic proteins (BMPs) are the best-characterized cytokines that drive osteogenic differentiation [5,6].

The BMPs, although historically named because of their potent ability to induce ectopic osteogenic differentiation in vivo [7,8], function in a wide variety of cell types to regulate many additional events associated with morphogene-sis, such as dorsal-ventral patterning during embryogenesis and the development of heart, lung, and kidney [9–13]. The BMPs belong to the transforming growth factor-β (TGF-β) family, and, thus, exert their biological function through forming a complex with type I and II serine/threonine kinase receptor, which in turn phosphorylates receptor mediated SMA/mothers against decapentaplegic (R-SMAD), including SMAD1, 5, 8. Activated SMAD1/5/8 form a complex with SMAD4 that subsequently translocates into the nucleus [14,15] where it cooperates with other DNA binding proteins to target specific genes for transcriptional regulation. The direct implications of these transcriptional events is best understood in the context of bone development, where it has been shown that the osteogenic-lineage-specific transcription factors distal-less homeobox *(Dlx)-2/5* [16–18] and runt-related transcription factor 2 *(Runx2)*/core binding factor α-1 *(cbfa-1)* [19,20] can be induced by BMPs to stimulate the expression of osteogenic-related genes, such as alkaline phosphatase

Department of Bioengineering, University of Pennsylvania, Philadelphia, Pennsylvania.
*Current affiliation: Department of Medicine, Skeleton Joint Research Center, National Cheng Kung University Medical College, Tainan, Taiwan.
†These two authors contributed equally to this work.

(ALP), type I collagen, bone sialoprotein, osteocalcin, and osteopontin [18,21–23]. Among the BMPs, BMP-2 is perhaps most well studied in the context of osteogenesis, and has been shown to promote bone repair in animal models in vivo [24]. However, the performance of BMPs decreases as one moves from rodents to higher mammals, and the successful rate of BMPs in human clinical studies has not been impressive [25–27]. It has been reported that at high seeding density in vitro, BMP-2 induces osteogenesis in rodent osteogenic stem cells but not in human cells [28], thus raising the possibility that additional factors are needed for BMP function in humans.

Adherent cells such as hMSCs generally require adhesion to an extracellular matrix (ECM) via integrins for many cellular functions, including differentiation, proliferation, survival, and migration [29]. Though not yet reported for BMPs, studies have implicated the need for particular ECMs and integrins for a large variety of growth factors to trigger appropriate responses, including EGF, PDGF, VEGF, and bFGF, among others [30–34]. However, normal bone development in vivo and the differentiation of osteogenic lineages in vitro appear to be influenced by specific ECM proteins and integrins [35,36]. Interestingly, integrin ligation is not the only adhesive requirement for osteogenic differentiation. When exposed to a dexamethasone-based mixture optimized for osteogenesis in culture, we previously reported that the physical spreading and flattening of hMSCs against the ECM during cell adhesion is also necessary to support the differentiation of hMSCs to an osteogenic fate [37]. This cell shape requirement appeared to modulate hMSC differentiation through a pathway involving the small GTPase, RhoA, which has been identified to regulate the differentiation of several cell types [38–40]. Despite these findings, since bone development in vivo arises from multiple distinct pathways and dexamethasone-induced and BMP-induced osteogenesis in culture may arise via distinct mechanisms, cell adhesion has not been considered critical to BMP signaling in general or BMP-induced osteogenesis in particular. As such, the requirements for cell shape and RhoA may be limited to in vitro, dexamethasone-induced osteogenic differentiation.

In this study, we examined whether cell adhesion can modulate the effects of BMP-2 in hMSCs during early stages of commitment toward an osteogenic lineage, and identify cell shape as a key regulator of BMP signaling and BMP-induced osteogenic differentiation of hMSCs. We demonstrate that BMP activates RhoA, Rho-associated protein kinase (ROCK), and cytoskeletal tension, and this activation depends on cell shape. Further, ROCK activity and associated cytoskeletal tension regulates hMSC commitment to BMP-induced osteogenic phenotype. This study highlights the role of cell adhesion in regulating BMP signaling, and provides a mechanism by which the changes in cell adhesion, shape, and mechanics present during morphogenesis can modulate cell differentiation.

Materials and Methods

Cell culture and reagents

hMSCs were obtained from Lonza Walkersville, Inc., and maintained in DMEM containing 10% fetal bovine serum, 0.3 mg/mL glutamine, 100 mg/mL streptomycin, and 100 U/mL penicillin. Only early passage (passage 4–6)

hMSCs were used in experiments. To induce osteogenesis, hMSCs were plated on fibronectin-coated (25 μg/mL) plates and treated with BMP-2 (100 ng/mL; R&D Systems) for 2 weeks. Treatment of cells with 0.1% bovine serum albumin served as a negative control. Media were changed every 3 days. Cells were then harvested for ALP staining, western blot, or real-time RT-PCR to detect the expression of osteogenic markers. SMAD4, SMAD1, and SMAD1 phosphorylation antibodies for immunoprecipitation or western blot are from Cell Signaling Technology

Generating micropatterned substrates

The microcontact printing technique used to fabricate substrates patterned with regions of ECM was created as previously described [41]. Briefly, polydimethyl siloxane (PDMS) stamps were made by casting Sylgard 184 (Dow Corning) liquid prepolymer over the silicon master. Upon curing, the elastomeric stamp was peeled off, washed with ethanol, and dried under nitrogen. Stamps were coated with fibronectin, thoroughly rinsed with deionized water, blown dry under nitrogen, and placed in conformal contact with a flat PDMS substrate. This substrate was blocked with 0.2% Pluronic F127 (BASF) and used under standard culture conditions.

Cell staining

ALP activity was assayed using Sigma kit No. 85 as per manufacturer's instructions. Cells were photographed and counted using a Nikon Eclipse TE200. For total cell counts, nuclei were stained with DAPI. For quantification of F-actin, cells were fixed, permeablized, and incubated with phalloidin-Alexa 568 (Invitrogen). The actin-bond phalloidin was extracted with methanol, and the fluorescent intensity was measured. The fluorescent readout was normalized with DNA amount, measured by CyQUANT cell proliferation assay kit (Invitrogen).

For immunofluoroscence labeling, cells were fixed in 4% paraformaldehyde followed by permeablization in 0.3% Triton X-100. Cells were incubated in 10% goat serum and then incubated in primary antibody followed by secondary antibody conjugated with Alexa-594. Actin cytoskeleton was stained with phalloidin-Alexa 488 (Invitrogen), and nuclei were stained with DAPI. Images were acquired by Zeiss Axiovert 200M and analyzed by AxioVision Rel. 4.7 analysis software (Zeiss).

Real-time RT-PCR analysis

Total RNA was isolated from cells grown in 60-mm dishes by using RNeasy Mini Kit as specified by the manufacturer (Qiagen). About 0.5 μg of total RNA was reverse transcribed by using MMLv reverse transcriptase as per manufacturer's instructions (Invitrogen). Real-time PCR was performed and monitored by using an ABI 7300 system (Applied Biosystems, Life Technologies). cDNA was analyzed by commercially available primers and probes from ABI [distal-less homeobox 5 (Dlx-5), Product No. Hs00193291_m1; Runx2, Product No. Hs00231692_m1; ALP, Product No. Hs01029144_m1] (Applied Biosystems) following the manufacturer's instructions. PCR was also performed with human GAPDH primers (Product No. Hs99999905_m1) for

normalization of the samples. cDNA was analyzed for the genes of interest and the housekeeping gene in independent reactions. Data analysis was performed using the ABI Prism 7300 Sequence Detection Systems version 1.0 software (Applied Biosystems).

Rho GTPase assay

Changes in the activation state of RhoA were determined according to the method of Ren and Schwartz [42,43] by isolating the GTP-bound RhoA in cell lysate with agarose beads conjugated to glutathione-S-transferase fused to the Rho binding domain Rhotekin (Upstate Biotechnology, Millipore). After washing, the beads were mixed with SDS sample buffer, boiled, and resolved by western blot. GTP-bound RhoA was detected by using monoclonal antibody to RhoA (Santa Cruz Biotechnology) followed by an HRP-labeled secondary antibody (Jackson ImmunoResearch Laboratories). Blots were developed by using ECL (GE Health Care Life Sciences). The amount of GTP-bound RhoA was normalized to the total amount of RhoA in cell lysates by using a digital imaging system (VersaDoc).

Measurement of traction forces

Microfabricated postarray detectors (mPADs) were used to measure traction forces, and fabricated as previously described [41,44]. mPADs used in these studies were 9 μm tall and 3 μm in diameter, with 9 μm center–center spacing. To control cell spreading on microneedle tips, the tips were stamped with fibronectin using microcontact printing [41], and nonstamped regions were blocked with 0.2% Pluronic F127 (BASF). For the live cell recording, hMSCs were cultured on mPAD and serum starved for overnight. Images were recorded 7 min before we added BMP (100 ng/mL) or bovine serum albumin as a control. Images were taken by 1 min interval and were taken for another 30 min after treatment. For end-point measurement, hMSCs were cultured on the mPADs, serum starved overnight, and treated with BMP-2 for 24 h. Samples were fixed and stained, and the images were taken by Axiovert 200M (Carl Zeiss MicroImaging, Inc.). Matlab (The MathWorks) was used to obtain traction force from the acquired images as previously described [41]. Overall, 50 control cells, 42 BMP-treated cells, and 17 BMP + Y27632-treated cells from 3 independent experiments were used for the force measurements.

Transfection of small-interfering RNA

The small-interfering RNA (siRNA; ON-TARGETplus®) that were specific to the target genes were purchased from Thermo Scientific/Dharmacon RNAi Technologies. The siRNA was transfected into hMSC by using Lipofectamin RNAiMAX® reagent (Invitrogen) according to the manufacturer's instructions.

Results

BMP-2-induced osteogenic differentiation is regulated by cell shape

We first examined whether adhesion modulates BMP-induced osteogenesis by first varying hMSC seeding density to manipulate adhesion. hMSCs were seeded at different densities (from 1,000 to 20,000 cells/cm², Fig. 1A, B) on fibronectin-coated dishes, and treated with BMP-2 (100 ng/mL) for 2 weeks. At the lowest seeding density, cells attached and spread with little contact between neighboring cells. At high seeding density, cells were confluent, and were physically constrained from spreading on the substrate due to cell crowding. The extent of osteogenesis was initially analyzed by staining for ALP activity. By 2 weeks, ALP activity dramatically increased for cells at low density, but remained at basal levels for cells at high density (Fig. 1A, B) after BMP treatment. Cells treated with different concentrations of BMP-2 (from 0 to 500 ng/mL) exhibited a dose-dependent induction of ALP activity in cells seeded at low but not high density (Fig. 1C). This density-dependent osteogenic differentiation was not unique to BMP-2, as this response also occurred with BMP-4 (data not shown). Since ALP staining alone was not diagnostic for osteogenesis, we performed real-time PCR on 2-week cultures to detect the expression level of several osteogenic markers known to be downstream of BMP-2 signaling including Dlx-5, cbfa-1/runx2, and ALP. BMP-2 induced increased expression of all 3 markers relative to untreated controls at low but not high cell density, thus confirming that BMP-2-induced osteogenesis depends on cell density (Fig. 1D). As expected, markers of end-stage osteogenic differentiation were not observed given that supplements such as 2-glycerophosphate and ascorbic acid-2-phosphate were not included in this study (to prevent confounding of the specific effects of BMP examined here).

Increasing cell seeding density not only increases cell-cell adhesion and paracrine signaling but also decreases cell spreading against the underlying matrix. To investigate whether the degree of cell spreading against the substrate alone can modulate BMP-2-induced osteogenesis, we used microcontact printing to generate substrates micropatterned with square islands of fibronectin such that single cells would attach and spread to the size of the islands [37,45]. hMSCs were seeded onto adhesive islands of different sizes (625–10,000 μm²) to control the degree of cell spreading in the presence or absence of BMP-2 (Fig. 1E, F) and after 2 weeks, cells were assessed for ALP activity. ALP activity was up-regulated in hMSCs that were well spread on large islands (10,000 μm²) but not in cells that remained unspread on small islands.

To further investigate how cell shape regulated BMP signaling and resultant osteogenic gene expression, we expressed in hMSCs a luciferase reporter driven by the Id-1 promoter, which contains a SMAD binding element (SBE) responsive to BMP treatment [46]. hMSCs expressing this SBE-luciferase reporter exhibited a dose-dependent luciferase response to increasing BMP-2 (from 0 to 300 ng/mL) (Supplementary Fig. S1; Supplementary Data are available online at www.liebertonline.com/scd). Using this system, we next examined whether reporter activity was regulated by cell shape. Indeed, SBE activity increased with BMP treatment only at low cell seeding densities (Fig. 1G), and showed a robust response on large (10,000 μm²) but not small (2,500; 625 μm²) micropatterned islands (Fig. 1H). We have previously reported that cell shape can regulate osteogenesis in a dexamethasone-containing osteogenic medium. Interestingly, although BMP stimulated robust SBE activity only in spread cells, dexamethasone did not impact SBE activity in either spread or unspread conditions (Supplementary Fig.
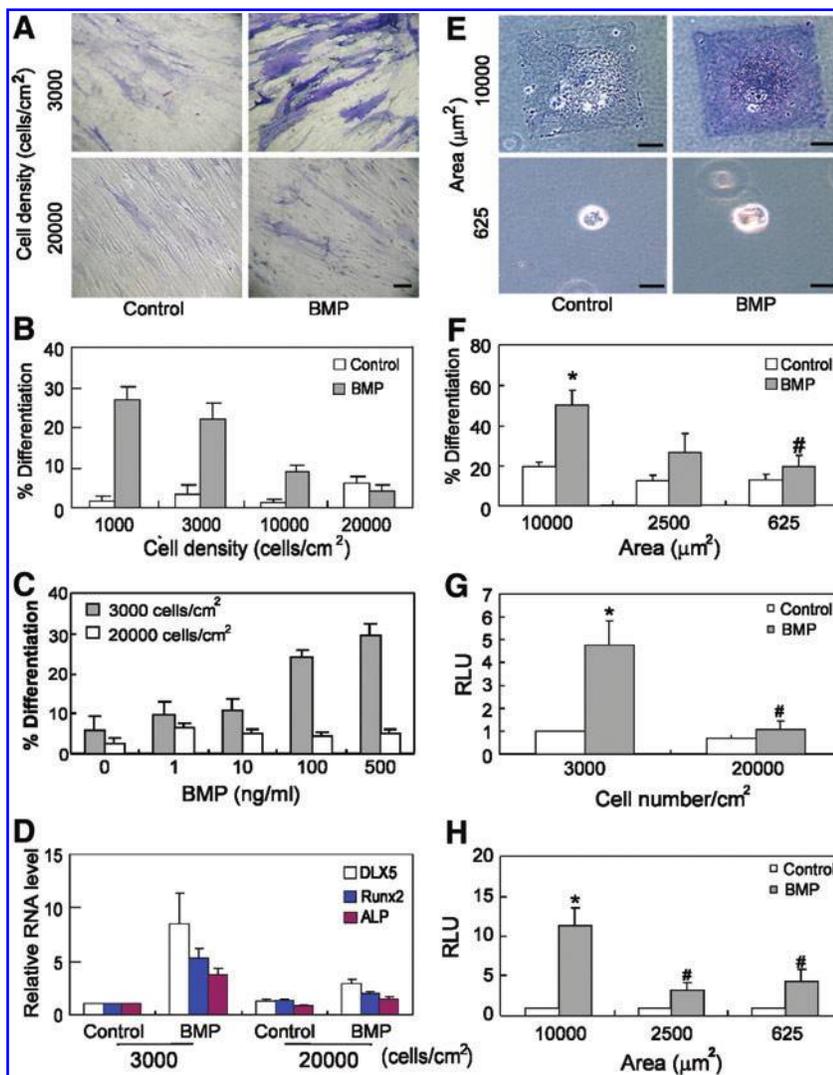
FIG. 1. BMP-2-induced osteogenic differentiation is regulated by cell shape. **(A)** Bright-field images of hMSC plated at 3,000 cells/cm^2 (*upper 2 panels*) or 20,000 cells/cm^2 (*lower 2 panels*), cultured for 2 weeks in the absence (*left panels*, Control) or presence (*right panels*, BMP) of BMP-2 (100 ng/mL), and stained with ALP activity. Scale bar: 20 μm. **(B)** Quantification plot of ratio of ALP positively stained cells versus DAPI-stained cells in 5 random selected fields of cultured cells at 1,000, 3,000, 10,000, and 20,000 cells/cm^2 in the absence or presence of BMP-2 (100 ng/mL). **(C)** Quantification of ratio of ALP positively stained hMSCs versus DAPI-stained cells in 5 random selected fields of cells cultured at 3,000 or 20,000 cells/cm^2 in the absence or presence of BMP-2 at different concentration (from 0 to 500 ng/mL). **(D)** Quantitative PCR results of osteogenic differentiation markers of hMSCs plated at indicated density and cultured in the absence or presence of BMP-2 (100 ng/mL) for 2 weeks. **(E)** Bright-field ALP images of hMSCs plated on large (10,000 μm^2, *upper panels*) or small (625 μm^2, *lower panels*) fibronectin islands for 2 weeks in the absence or presence of BMP-2 (100 ng/mL). Scale bar: 20 μm. **(F)** Quantification plot of ratio of ALP positively stained cells versus DAPI-stained cells plated on different sizes of fibronectin stamped areas (from 625 to 10,000 μm^2) in the absence or presence of BMP-2. **(G)** Luciferase activity of SBE-luciferase transfected hMSCs plated at 3,000 cells/cm^2 or 20,000 cells/cm^2 in the presence or absence of BMP-2 (100 ng/mL) for 2 days. **(H)** Luciferase activity of SBE-luciferase transfected hMSCs cultured on fibronectin micropattern stamped spread (10,000 μm^2) or unspread (625 μm^2) followed by treatment with BMP-2 (100 ng/mL) for 2 days. All quantification data were presented as mean ± SEM of at lease 3 independent experiments. *$P < 0.05$ versus paired control; #$P < 0.05$ versus low density/spread cells treated with BMP-2. ALP, alkaline phosphatase; BMP-2, bone morphogenetic protein; hMSC, human mesenchymal stem cells; SBE, SMAD binding element; SMAD, SMA/mothers against decapentaplegic. Color images available online at www.liebertonline.com/scd

S2). Together, these results suggest that cell shape regulates BMP-induced osteogenesis in hMSCs, and that this effect could be exerted by cell shape regulation of SMAD1/5/8 signaling, a mechanism distinct from our previous reports.

BMP stimulates RhoA/ROCK signaling and increases cytoskeletal tension

We previously implicated RhoA in dexamethasone-induced hMSC commitment to an osteogenic lineage [37]. Hence, it is possible that BMP-induced osteogenesis may also involve RhoA. To explore this possibility, we first investigated whether BMP treatment activates RhoA by using the pull-down assay [42,43]. In hMSCs seeded at low density, BMP-2 treatment increased in RhoA activity within 20 min. This activity peaked after 1 h, dropped down to basal after 8 h (Fig. 2A). Interestingly, this activation was absent in cells

seeded at high density after 1 hr BMP treatment (Fig. 2B). Consistent with an increase in RhoA activity, we observed that BMP-2 significantly increased kinase activity of the RhoA effector, ROCK, at low but not high cell density, using immunoprecipitated ROCK from cell lysates and recombinant MYPT1 as a kinase substrate (Fig. 2C). To confirm the BMP-induced RhoA/ROCK signaling, we also measured levels of phosphorylated myosin light chain (ppMLC) by western blotting. BMP-2 treatment increased ppMLC levels only in cells seeded at low density (Fig. 2D).

These data suggested that BMP induces Rho/ROCK-mediated myosin activity, and indirectly suggested that BMP triggered cytoskeletally generated contractile tension in hMSCs. Indeed, we observed that BMP-2 treatment increased the formation of actin stress fibers at low cell seeding density, but not at high seeding density (Fig. 3A, B). We then directly measured traction forces in BMP-treated hMSCs by
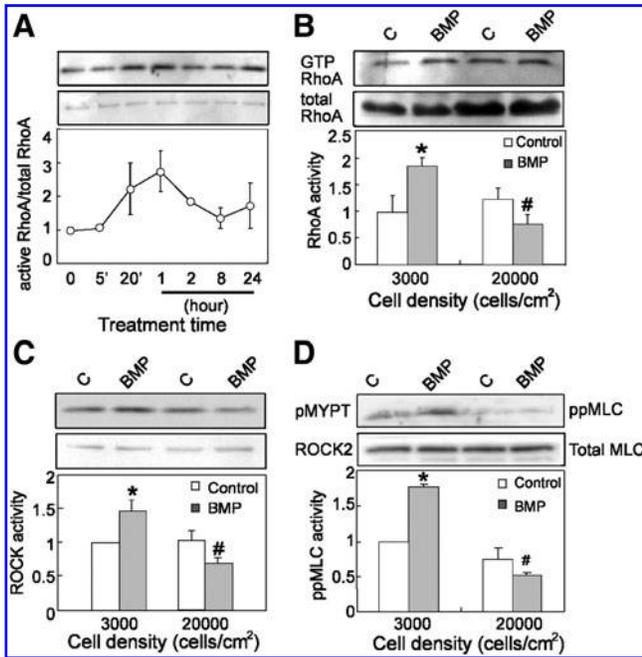
FIG. 2. BMP stimulates RhoA signaling. (A) Western blot (*upper panels*) and quantification plot (*lower panel*) showed active RhoA in serum-starved hMSCs at 3,000 cells/cm² with BMP-2 (100 ng/mL) treatment at different time points. (B) Western blot and quantification plot showed active RhoA in serum-starved hMSCs plated at 3,000 or 20,000 cells/cm² with or without BMP-2 (100 ng/mL) treatment. (*$P < 0.05$ vs. paired control; #$P < 0.05$ vs. BMP treatment at 3,000 cells/cm²). (C) Western blot and quantification plot showed levels of recombined p-mypt after in vitro ROCK kinase assay in serum-starved hMSCs plated at 3,000 or 20,000 cells/cm² with or without BMP-2 (100 ng/mL) treatment. (*$P < 0.05$ vs. paired control; #$P < 0.05$ vs. BMP treatment at 3,000 cells/cm²). (D) Western blot ppMLC/MLC and quantification plot showed activation of ppMLC in serum-starved hMSCs plated at 3,000 or 20,000 cells/cm² with or without BMP-2 (100 ng/mL) treatment (*$P < 0.05$ vs. paired control; #$P < 0.05$ vs. BMP treatment at 3,000 cells/cm²). All western blot results were presented as a representative experiment of at least 3 independent experiments. ppMLC, phosphorylated myosin light chain. ROCK, Rho-associated protein kinase.

using a previously described microfabricated force sensor [41]. hMSCs were seeded on the force sensors and then exposed to BMP-2. Indeed, BMP treatment rapidly increased traction force within 10 min of exposure (Supplementary Movie S1) and lasted for 24 h (Fig. 3C). Further, this traction force was ROCK dependent, as the ROCK inhibitor Y27632 blocked the BMP-induced stress fiber formation and force generation (Fig. 3C, D).

BMP-induced osteogenesis is ROCK and tension dependent

Although RhoA/ROCK/myosin activity increased on BMP treatment, it remained unclear whether this increase was relevant to BMP-induced osteogenesis. To test this possibility, hMSCs were treated with either the ROCK inhibitor Y27632 (10 μM) or nonmuscle myosin II inhibitor blebbistatin (25 μM) in the presence of BMP-2. Both Y27632 and blebbistatin abrogated BMP-2-induced osteogenesis (Fig.
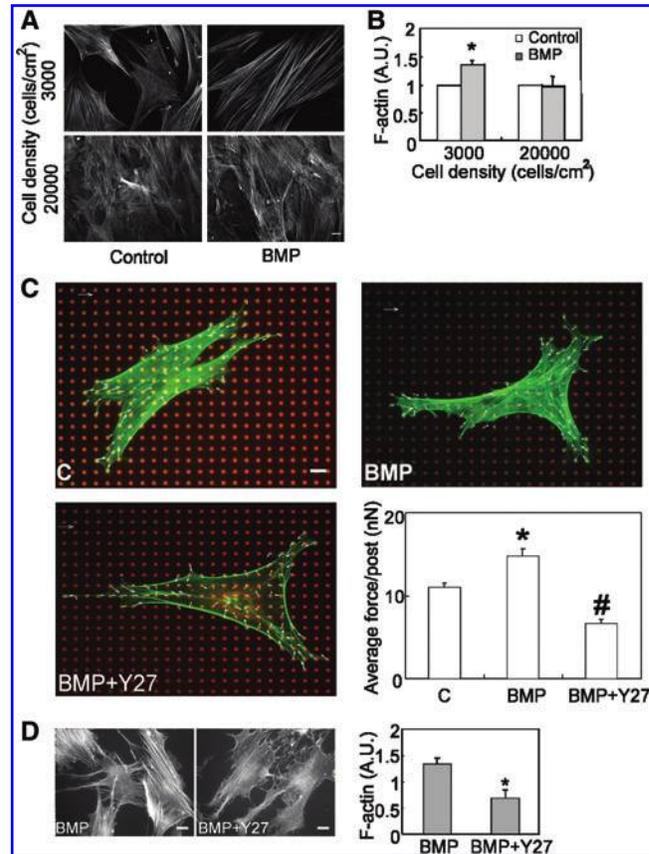
FIG. 3. BMP stimulates cytoskeletal tension. (A) Epifluorescence images of stress fibers in hMSCs plated at 3,000 (*upper panels*) or 20,000 (*lower panels*) cells/cm² in the absence (*left panels*, Control) or presence of BMP-2 (*right panels*, BMP, 100 ng/mL) for 1 h. (B) Quantification results of stress fiber formation in hMSCs plated at 3,000 or 20,000 cells/cm² in the absence or presence of BMP-2 (100 ng/mL) (*$P < 0.05$ vs. paired control.). A.U. represents arbitrary unit. (C) Representative images of control (C), BMP-2 (100 ng/mL) (BMP) and BMP-2 plus Y27632 (25 μM) (BMP + Y27) treated hMSC on mPAD (red, mPAD; green, actin cytoskeleton; blue, nuclei). Plot of average traction force exerted on each underlying post were presented as mean ± SEM of 3 independent experiments (*$P < 0.01$ vs. C; #$P < 0.01$ between BMP-2 and BMP-2 + Y27). Scale bar: 20 μm. (D) Fluorescence images and quantification plot of stress fibers in hMSCs plated at 3,000 cells/cm² and treated with Y27632 (10 μM) in the presence of BMP-2 (100 ng/mL) for 1 h. mPAD, microfabricated postarray detector. Color images available online at www.liebertonline.com/scd

4A, B). Since the pharmacological inhibitors could exert nonspecific or off-target effects, we also knocked down ROCK by using siRNA, BMP induced robust activation of ALP activity in siGlo, and untreated (no siRNA) control cells (Fig. 4C, D). Knockdown of BMP receptor type II and BMP-induced osteogenic transcription factors Runx2 and Dlx-5 resulted in the downregulation of BMP-induced ALP activity, serving as positive controls for the approach. Importantly, knockdown of either ROCK I or ROCK II decreased BMP-induced ALP activity (Fig. 4C, D). Taken together, these data indicate that BMP-2 signaling triggers RhoA/ROCK activation and that this event is required for BMP-2-induced osteogenesis.
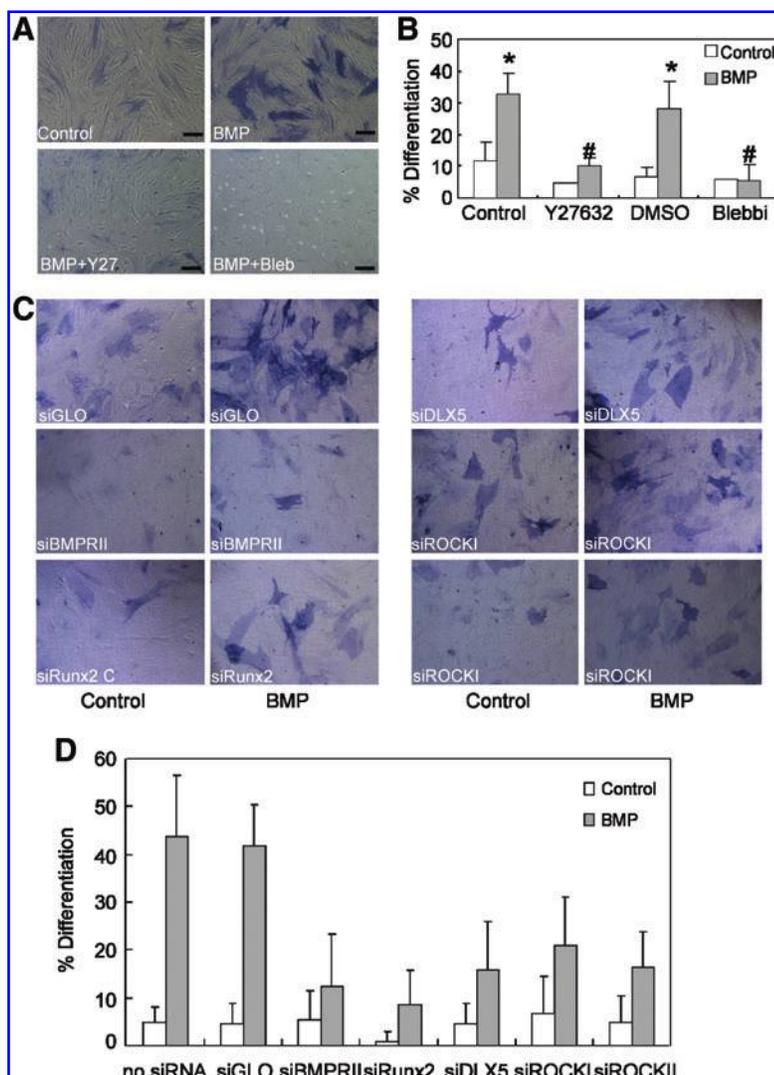
FIG. 4. BMP-induced osteogenic differentiation depends on ROCK and myosin activity. **(A)** Bright-field images of hMSC plated at 3,000 cells/cm^2 for 2 weeks in the absence (Control) or presence of BMP-2 (100 ng/mL), BMP-2 plus Y27632 (BMP+Y27, 10 μM), and BMP-2 plus blebbistatin (BMP+Bleb, 25 μM) and stained with ALP activity. Scale bar: 20 μm. **(B)** Quantification plot of ratio of ALP positively stained hMSCs versus DAPI-stained cells in 5 random selected fields as indicated. All results were presented as mean±SEM (*$P < 0.05$ vs. paired control; #$P < 0.05$ vs. paired BMP only). **(C)** Bright-field images of hMSC with knock down of specific gene using small-interfering RNA (as indicated) and plated at 3,000 cells/cm^2 for 2 weeks in the absence (Control) or presence of BMP-2 (BMP, 100 ng/mL) and stained with ALP activity. **(D)** Quantification plot of ratio of ALP positively stained hMSCs versus DAPI-stained cells in 5 random selected fields as indicated. Color images available online at www.liebertonline.com/scd

BMP-induced SMAD1/5/8 phosphorylation is regulated by ROCK and myosin signaling

To examine whether the BMP-induced increase in RhoA/ROCK/myosin that occurs only in spread cells is involved in regulating transcriptional activity of the SBE, we first examined SBE-luciferase activity in hMSCs after inhibition of ROCK activity. Treatment with Y27632 suppressed BMP-2-mediated reporter activity (Fig. 5A). Further, treatment with blebbistatin blunted BMP-2-induced increase of SBE-luciferase activity (Fig. 5B). These results suggest that the requirement for cell spreading and ROCK/myosin signaling in BMP-induced signaling and osteogenesis likely occurs upstream of activation of the SBE.

Since SMAD-mediated gene transcription requires SMAD phosphorylation, complex formation with SMAD4, and translocation of the complex into the nucleus [47], we tested whether ROCK/myosin signaling was required for each of these steps. To examine SMAD phosphorylation, cells were pretreated with Y27632 (10 μM) or blebbistatin (25 μM) and then stimulated with BMP-2 for 1 h, and then the levels of p-SMAD1/5/8 were examined by western blotting. Although SMAD1/5/8 was efficiently phosphorylated in response to

BMP-2 treatment (Fig. 6A), treatment of either Y27632 or blebbistatin antagonized this effect (Fig. 6A, B).

To examine whether ROCK/myosin signaling was required for SMAD complex formation, hMSCs again were pretreated with Y27632 (10 μM) or blebbistatin (25 μM), exposed to BMP-2 for 1 h, and then lysates were immunoprecipitated with anti-SMAD4 antibody followed by immunoblotting with p-SMAD1/5/8 antibody. Exposure to BMP increased immunoprecipitation of SMAD4 with SMAD1/5/8, whereas treatment with either Y27632 or blebbistatin abrogated the BMP-2 induced formation of p-SMAD/SMAD4 complex (Fig. 6C–F).

We next examined whether SMAD nuclear localization was impacted by cell shape or ROCK signaling. In the absence of BMP treatment in the hMSCs, only a small amount of p-SMAD1/5/8 could be detected in hMSCs by immunofluorescence. However, after 1 h of BMP treatment, p-SMAD1/5/8 was highly enriched in the nuclei of well-spread cells (Fig. 7A, upper panels, B). Further, as the degree of cell spreading decreased by plating on smaller micro-patterned islands, the amount of nuclear localization of p-SMAD1/5/8 decreased (Fig. 7A, B). To examine whether ROCK signaling was involved in this cell shape regulation of

FIG. 5. SMAD-dependent gene expression is regulated by ROCK and myosin activity. **(A)** Luciferase activity of SBE-luciferase-transfected hMSCs plated at 3,000 cells/cm^2 and in the absence or presence of BMP-2 (100 ng/mL) or Y27632 (10 μM) for 2 days. **(B)** Luciferase activity of SBE-luciferase transfected hMSCs plated at 3,000 cells/cm^2 and in the absence or presence of BMP-2 (100 ng/mL) or blebbistatin (25 μM) for 2 days. Cotransfection of renilla-luciferase served as an internal control. All data were presented as mean ± SEM. *$P < 0.05$ versus paired control; #$P < 0.05$ versus treated with BMP-2.
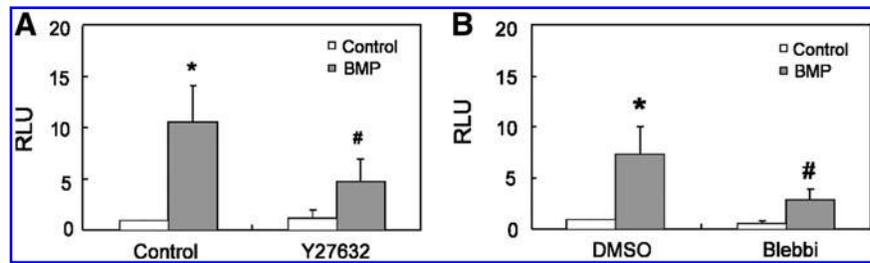

BMP-induced SMAD nuclear translocation, cells were pretreated with Y27632 (25 μM) or blebbistatin (25 μM) 1 h before stimulation by BMP-2. Indeed, blocking ROCK/myosin signaling in well-spread cells also blocked nuclear localization of p-SMAD (Fig. 7C, D). Together, these findings suggest a novel control point in regulating BMP signaling, through modulation of SMAD signaling by cell shape, ROCK, and cytoskeletal tension.

Discussion

BMPs are considered one of the most important and potent classes of morphogens in early development. They also have a classical and important role in osteogenesis throughout life, and appear to be powerful inducers of osteogenic differentiation in cultures of MSCs derived from many animals [48]. Interestingly, although cell adhesion to the ECM has been shown to regulate cellular responses from many cytokines such as EGF, PDGF, bFGF, and VEGF [30–34], no molecular link between adhesive cues and BMP signaling has been established. We now show that the degree of cell adhesion and spreading against ECM substrate can regulate BMP-induced SMAD signaling and downstream

gene transcription, and does so through cross-talk with the RhoA/ROCK signaling pathway (Fig. 7C). This adhesion- and spreading-dependent regulation of BMP-signaling is not only relevant in the context of early osteogenic differentiation but also appears to be a more general mechanism, as it also extends to other cell types (Supplementary Fig. S3). Previous studies have demonstrated a role for cell adhesion and associated changes in cell shape in regulating numerous cell functions including proliferation, apoptosis, and differentiation [37,45,49–52]. The involvement of cell shape in BMP signaling, in particular, given the central role of BMPs to development, may provide an important mechanism linking the structural changes of morphogenesis to specific differentiation events during tissue development. For example, we would speculate that the rounded phenotype of chondrogenic progenitors at articular joints or adipogenic precursors within marrow may, in fact, protect them from undergoing an osteogenic response when exposed to local BMP gradients. Beyond developmental contexts, understanding how BMP regulates MSC differentiation is critically important for developing clinical therapies for nonunion fractures [53]. Although BMP-2 and BMP-4 are widely used as osteoinductive treatments during surgical repair of bone, the success rate of

FIG. 6. BMP-induced phosphorylation of SMAD and SMAD complex formation is ROCK and tension dependent. **(A)** A representative western blot result of levels of p-SMAD1/5/8 in hMSC plated at 3,000 cells/cm^2 in the absence or presence of BMP (100 ng/mL), BMP + Y27632 (BMP + Y27, 10 μM), BMP + blebbistatin (BMP + Bleb, 25 μM), Y27632 (Y27, 10 μM), and blebbistatin (Bleb, 25 μM). GAPDH served as an internal control. **(B)** Quantification plot of ratio of pSMAD1/5/8 levels of **(A)**. **(C, E)** Cell lysates from different treatments were immunoprecipitated with anti-SMAD4 followed by immunoblotting with either anti-p-SMAD1 or SMAD4 antibodies. **(D, F)** Quantification results of immunoprecipitated pSMAD1 with SMAD4 in MSC treated with either Y27632 (10 μM) **(D)** or blebbistatin (25 μM) **(F)**.
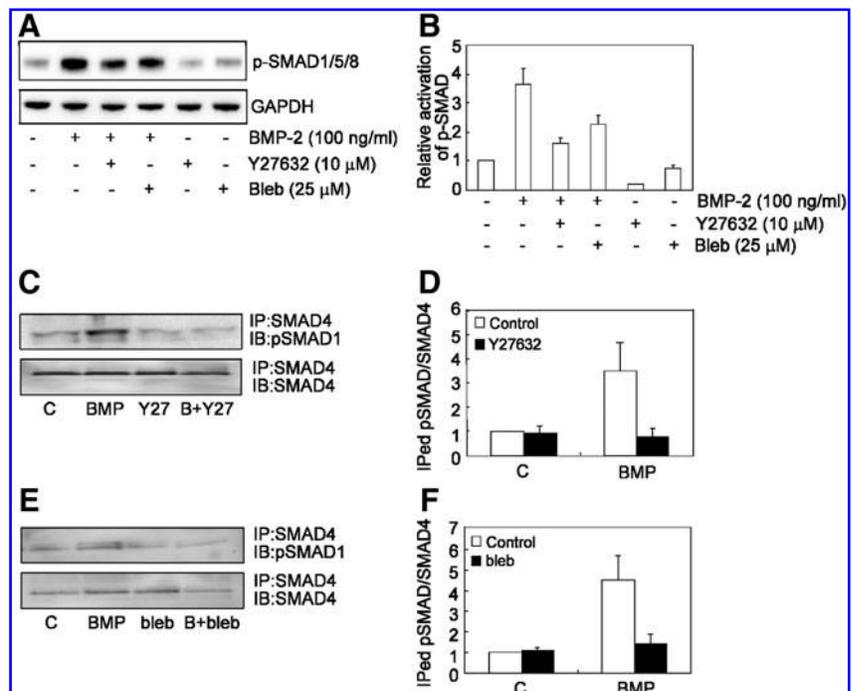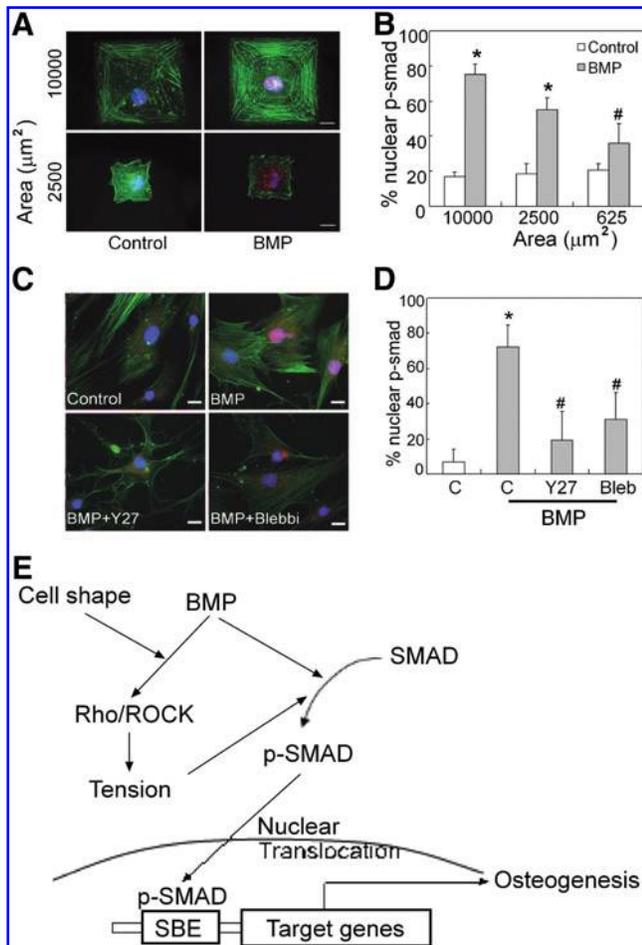
FIG. 7. p-SMAD1/5/8 nuclear translocation requires cell spreading and ROCK signaling. **(A)** Immunofluorescence images of serum-starved hMSCs plated on fibronectin stamped islands and treated with or without BMP-2 (100 ng/mL) for 1 h. Green, stress fiber; red, p-SMAD1/5/8; blue, DAPI. **(B)** Quantification of ratio of nuclear translocated p-SMAD1/5/8 in hMSCs plated on different sizes of fibronectin-stamped area. **(C)** Immunofluorescence images of Y27632 (10 μM) or blebbstatin (25 μM) pretreated hMSCs followed by BMP treatment for 1 h. Green, stress fiber; red, p-SMAD1/5/8; blue, DAPI. **(D)** Quantification of BMP-2-induced nuclear translocated p-SMAD1/5/8 in the presence of Y27632 or blebbstatin. *$P < 0.05$ versus paired control; #$P < 0.05$ versus BMP-treatment at 10,000 μm^2 and BMP treat alone. Scale bar, 20 μm. **(E)** Model of cell shape regulates BMP-2-induced osteogenic differentiation. Cell shape acts as a mechanical cue that cooperates with BMP to induced osteogenesis. Rho/ROCK-mediated cell tension is not only required but also induced in response to BMP-2 treatment. The RhoA/ROCK signaling regulates nuclear translocation of p-SMAD, which is responsible for BMP-2 induced osteogenesis.

BMP as a therapeutic intervention is highly variable [25–27]. It is interesting to speculate that a limiting factor in these environments is the lack of an appropriate adhesive setting to allow BMP-stimulated cells to mount a contractile response. The inflammatory environment and the disruption of normal ECM proteins may contribute to poor cell adhesion and/or spreading, thereby limiting the efficacy of BMP treatments to promote bone growth and healing. Our studies suggest that

controlling the mechanical responses of cells at these wound sites may be an important factor controlling the overall osteoinductive properties of BMPs. Such control mechanisms underscore the importance of the adhesive microenvironment in regulating stem cell differentiation. Indeed, the elaboration of ECM during osteogenesis is critical for bone development [54,55].

Although the mechanical activity of MSCs has not been studied in vivo, it has been reported that continuous delivery of the ROCK inhibitor Y27632 to mice enhanced BMP-2 dependent bone formation [56]. Although this study would seem to contradict our current observations, it is important to note that there may be species differences in the mechanical dependence of osteogenesis [28], and this study did not investigate whether the bone formation occurred through an endochondral versus intramembraneous route. Since Y27632 is known to increase chondrogenic differentiation [57], it is possible that the observed effect in the murine system can be attributed to enhanced chondrogenesis and subsequent endochondral bone formation. In contrast, our study focused on direct osteogenic commitment, and would, therefore, anticipate that in vivo significance of the role of Rho-ROCK signaling in BMP-2 induced bone would be important specifically for intramembraneous bone formation.

The only identified substrate of BMP receptor kinases are the SMADs [58]. Nonetheless, recent evidence suggests that BMPs can also activate the MAP kinases through a SMAD- and transcription-independent pathway, though the molecular basis for this activation remains undefined [59,60]. Here, we showed that exposure to BMP ligands leads to rapid and sustained activation of RhoA. Since TGF-β can also stimulate RhoA [39], the connection to Rho GTPases may represent a general link that is conserved across several members of the TGF-β superfamily. Interestingly, several Rho GTPases family members appear to be required for diverse biological responses regulated by the TGF-β superfamily, including dendritogenesis in neurons, epithelial to mesenchymal transitions, and myofibrillogenesis [39,60,61]. In addition to the rapid activation, SMAD-dependent transcriptional effects could be involved in sustaining changes in Rho GTPases signaling. Indeed, TGF-β-induced regulation of cdc42 and RhoA signaling appears to be transcriptionally regulated [61]. Regardless of the mechanisms involved, this activation of RhoA by BMPs appears to have both biochemical and mechanical functions.

We previously reported that dexamethasone-driven osteogenesis was mediated by cell adhesion and RhoA activation [37]. Here, we show that cell adhesion, RhoA-mediated ROCK activity, and cytoskeletal tension are required for BMP-induced osteogenesis. Although one might conclude that these mechanical signals likely impact osteogenesis through a single common mechanism, our results suggest that dexamethasone does not induce Smad-mediated gene transcription. Indeed, comparisons between gene expression responses to BMP-versus dexamethasone-stimulated osteogenesis show little in common (Supplementary Fig. S2). Thus, these data indicate a distinct, newly identified interdependency between BMP and RhoA signaling.

BMP signaling appears not only to induce RhoA/ROCK signaling, but also to require it for downstream signaling by SMADs. On binding of BMP to its receptor, SMAD1/5/8 is phosphorylated, binds to SMAD4, and the complex

translocates into the nucleus where it exerts its transcriptional effects. A previous work had shown that TGF-β-induced SMAD2 phosphorylation is blocked when RhoA is antagonized [38]. Our data now show that RhoA signaling is necessary for BMP-induced SMAD1 phosphorylation, complex formation of phoshorylated SMAD1/5/8 with SMAD4, and subsequent nuclear translocation. One distinction is that TGF-β -induced nuclear translocation of SMAD2 is associated with microtubules, and did not implicate adhesion [62,63]. The primary mediator of RhoA's effects on microtubule dynamics is the effector diaphanous [62], whereas our studies demonstrate the involvement of ROCK and actin cytoskeletal tension. Thus, these data indicate distinct regulation of RhoA-regulated SMAD by BMP versus TGF-β. Previous studies have demonstrated a role for adhesion in redistributing MAPKs to the nucleus [63]. Despite the reported role for ERK and p38 in osteogenesis [57,63,64], we did not observe changes in ERK activation or p38 localization in our BMP-induced MSCs (data not shown). Nonetheless, regulation by RhoA/ROCK and actin cytoskeleton of transcriptional signals is not unique to the SMADs. Most notably, RelA and MRTF have been described to respond to these signals by yet other distinct molecular mechanisms [51, 65–67]. Thus, the demonstration here that cell shape can directly impact SMAD signaling illustrates one of the several mechanisms supporting the tight coupling by which cell structure regulates function. The link from RhoA signaling to transcription also provides a molecular basis for how other microenvironmental signals that converge on RhoA signaling could modulate differentiation programs through interactions with SMAD signaling.

The modulation of BMP signaling and SMAD-mediated gene expression occurs specifically through changes in ROCK activity and the downstream generation of cytoskeletal tension, and provides a molecular explanation for how mechanics can feed back to affect cell function. This link between cellular mechanics, signal transduction, and transcriptional regulation provides a means to begin to understand how mechanical conditions can specifically drive cell differentiation. Since BMPs are ubiquitous regulators of a myriad of cellular processes throughout development and adult life, these findings may, in fact, provide a more general model for how contractile forces can arise during development and translate to specific functions in vivo.

Acknowledgments

Author Disclosure Statement

The authors have declared that no competing interests exist.

References

1. Huang CY, KL Hagar, LE Frost, Y Sun and HS Cheung. (2004). Effects of cyclic compressive loading on chondrogenesis of rabbit bone-marrow derived mesenchymal stem cells. Stem Cells 22:313–323.
2. Hung SC, CF Chang, HL Ma, TH Chen and LT Ho. (2004). Gene expression profiles of early adipogenesis in human mesenchymal stem cells. Gene 340:141–150.
3. Meyers VE, M Zayzafoon, JT Douglas and JM McDonlad. (2005). RhoA and cytoskeletal disruption mediate reduced osteoblastogenesis and enhanced adipogenesis of human mesenchymal stem cells in modeled microgravity. J Bone Miner Res 20:1858–1866.
4. Pittenger MF, AM Mackay, SC Beck, RK Jaiswal, R Douglas, JD Mosca, MA Moorman, DW Simonetti, S Craig, and DR Marshak. (1999). Multilineage potential of adult human mesenchymal stem cells. Science 284:143–147.
5. Urist MR. (1965). Bone: formation by autoinduction. Science 150:893–899.
6. Reddi AH. (1998). Role of morphogenetic proteins in skeletal tissue engineering and regeneration. Nat Biotechnol 16: 247–252.
7. Wozney JM, V Rosen, AJ Celeste, LM Mitsock, MJ Whitters, RW Kriz, RM Hewick and EA Wang. (1988). Novel regulators of bone formation: molecular clones and activities. Science 242:1528–1534.
8. Urist MR, A Mikulski and A Lietze. (1979). Solubilized and insolubilized bone morphogenetic protein. Proc Natl Acad Sci U S A 76:1828–1832.
9. Schier AF and WS Talbot. (2005). Molecular genetics of axis formation in zebrafish. Annu Rev Genet 39:561–613.
10. Zhang H and A Bradley. (1996). Mice deficient for BMP2 are nonviable and have defects in amnion/chorion and cardiac development. Development 122:2977–2986.
11. El-Bizri N, C Guignabert, L Wang, A Cheng, K Stankunas, CP Chang, Y Mishina and M Rabinovitch. (2008). SM22alpha-targeted deletion of bone morphogenetic protein receptor 1A in mice impairs cardiac and vascular development, and influences organogenesis. Development 135:2981–2991.
12. Cain JE, S Hartwig, JF Bertram and ND Rosenblum. (2008). Bone morphogenetic protein signaling in the developing kidney: present and future. Differentiation 76: 831–842.
13. Luo G, C Hofmann, AL Bronckers, M Sohocki, A Bradley and G Karsenty. (1995). BMP-7 is an inducer of nephrogenesis, and is also required for eye development and skeletal patterning. Genes Dev 9:2808–2820.
14. Liu F, A Hata, J Baker, J Doody, J Carcamo and J Massague. (1996). A human Mad protein acting as a BMP-regulated transcriptional activator. Nature 381:620–623.
15. Massague J. (1998). TGF-beta signal transduction. Annu Rev Biochem 67:753–791.
16. Lee MH, YJ Kim, HJ Kim, HD Park, AR Kang, HM Kyung, JH Sung, JM Wozney, HJ Kim and HM Ryoo. (2003). BMP-2-induced Runx2 expression is mediated by Dlx5, and TGF-beta 1 opposes the BMP-2-induced osteoblast differentiation by suppression of Dlx5 expression. J Biol Chem 278:34387–34394.
17. Miyama K, G Yamada, TS Yamamoto, C Takagi, K Miyado, M Sakai, N Ueno and H Shibuya. (1999). A BMP-inducible gene, dlx5, regulates osteoblast differentiation and mesoderm induction. Dev Biol 208:123–133.
18. Ryoo HM, HM Hoffmann, T Beumer, B Frenkel, DA Towler, GS Stein, JL Stein, AJ van Wijnen and JB Lian.

(1997). Stage-specific expression of Dlx-5 during osteoblast differentiation: involvement in regulation of osteocalcin gene expression. Mol Endocrinol 11:1681–1694.

19. Lee KS, HJ Kim, QL Li, XZ Chi, C Ueta, T Komori, JM Wozney, EG Kim, JY Choi, HM Ryoo and SC Bae. (2000). Runx2 is a common target of transforming growth factor beta1 and bone morphogenetic protein 2, and cooperation between Runx2 and Smad5 induces osteoblast-specific gene expression in the pluripotent mesenchymal precursor cell line C2C12. Mol Cell Biol 20:8783–8792.

20. Wang Q, X Wei, T Zhu, M Zhang, R Shen, L Xing, RJ O'Keefe and D Chen. (2007). Bone morphogenetic protein 2 activates Smad6 gene transcription through bone-specific transcription factor Runx2. J Biol Chem 282: 10742–10748.

21. Kim YJ, MH Lee, JM Wozney, JY Cho and HM Ryoo. (2004). Bone morphogenetic protein-2-induced alkaline phosphatase expression is stimulated by Dlx5 and repressed by Msx2. J Biol Chem 279:50773–50780.

22. Liu T, Y Gao, K Sakamoto, T Minamizato, K Fukukawa, T Tsukazaki, Y Shibata, K Bessho, T Komori and A Yamaguchi. (2007). BMP-2 promotes differentiation of osteoblasts and chondroblasts in Runx2-deficient cell lines. J Cell Physiol 211:728–735.

23. Zhang YW, N Yasui, K Ito, G Huang, M Fujii, J Hanai, H Nogami, T Ochi, K Miyazono and Y Ito. (2000). A RUNX2/PEBP2alpha A/CBFA1 mutation displaying impaired transactivation and Smad interaction in cleidocranial dysplasia. Proc Natl Acad Sci U S A 97:10549–10554.

24. Lane JM. (2001). BMPs: why are they not in everyday use? J Bone Joint Surg Am 83-A Suppl 1:S161–163.

25. Valentin-Opran A, J Wozney, C Csimma, L Lilly and GE Riedel. (2002). Clinical evaluation of recombinant human bone morphogenetic protein-2. Clin Orthop Relat Res 395:110–120.

26. Boden SD. (2001). Clinical application of the BMPs. J Bone Joint Surg Am 83-A Suppl 1:S161.

27. Service RF. (2000). Tissue engineers build new bone. Science 289:1498–1500.

28. Diefenderfer DL, AM Osyczka, GC Reilly and PS Leboy. (2003). BMP responsiveness in human mesenchymal stem cells. Connect Tissue Res 44 Suppl 1:305–311.

29. Schwartz MA and MH Ginsberg. (2002). Networks and crosstalk: integrin signaling spreads. Nat Cell Biol 4:E65–E68.

30. Eliceiri B, R Klemke, S Strömblad and DA Cheresh. (1998). Integrin alphavbeta3 requirement for sustained mitogen-activated protein kinase activity during angiogenesis. J Cell Biol 140:1255–1263.

31. Weis S, J Lindquist, L Barnes, KM Lutu-Fuga, J Cui, MR Wood and DA Cheresh. (2006). Cooperation between VEGF and beta3 integrin during cardiac vascular development. Blood 109:1962–1970.

32. Ingber D and J Folkman. (1989). Mechanochemical switching between growth and differentiation during fibroblast growth factor-stimulated angiogenesis in vitro: role of extracellular matrix. J Cell Biol 109:317–330.

33. Hellman U, L Malm, LP Ma, G Larsson, S Mörner, M Fu, A Engström-Laurent and A Waldenström. (2010). Growth factor PDGF-BB stimulates cultured cardiomyocytes to synthesize the extracellular matrix component hyaluronan. PLoS One 5:e14393.

34. Maheshwari G, AM Wells, L Griffith and DA Lauffenburger. (1999). Biophysical integration of effects of epidermal growth factor and fibronectin on fibroblast migration. Biophys J 76:2814–2823.

35. Olsen BR, AM Reginato and W Wang. (2000). Bone development. Annu Rev Cell Dev Biol 16:191–220.

36. Salasznyk RM, WA Williams, A Boskey, A Batorsky and GE Plopper. (2004). Adhesion to vitronectin and collagen I promotes osteogenic differentiation of human mesenchymal stem cells. J Biomed Biotechnol 2004:24–34.

37. McBeath R, DM Pirone, CM Nelson, K Bhadriraju and CS Chen CS. (2004). Cell shape, cytoskeletal tension, and RhoA regulate stem cell lineage commitment. Dev Cell 6:483–495.

38. Sordella R, W Jiang, GC Chen, M Curto and J Settleman. (2003). Modulation of Rho GTPase signaling regulates a switch between adipogenesis and myogenesis. Cell 113: 147–158.

39. Chen S, M Crawford, RM Day, VR Briones, JE Leader, RA Jose and RJ Lechleider. (2006). RhoA modulates Smad signaling during transforming growth factor-beta-induced smooth muscle differentiation. J Biol Chem 281:1765–1770.

40. Arnsdorf EJ, Tummala P, Kwon RY and Jacobs CR. (2009). Mechanically induced osteogenic differentiation—the role of RhoA, ROCKII and cytoskeletal dynamics. J Cell Sci 122:546–553.

41. Tan JL, J Tien, DM Pirone, DS Gray, K Bhadriraju and CS Chen. (2003). Cells lying on a bed of microneedles: an approach to isolate mechanical force. Proc Natl Acad Sci U S A 100:1484–1489.

42. Ren XD, WB Kiosses and MA Schwartz. (1999). Regulation of the small GTP-binding protein Rho by cell adhesion and the cytoskeleton. EMBO J 18:578–585.

43. Ren XD and MA Schwartz. (2000). Determination of GTP loading on Rho. Methods Enzymol 325:264–272.

44. Lemmon CA, NJ Sniadecki, SA Ruiz, JT Tan, LH Romer and CS Chen. (2005). Shear force at the cell-matrix interface: enhanced analysis for microfabricated post array detectors. Mech Chem Biosyst 2:1–16.

45. Chen CS, M Mrksich, S Huang, GM Whitesides and DE Ingber. (1997). Geometric control of cell life and death. Science 276:1425–1428.

46. Korchynskyi O and P ten Dijke. (2002). Identification and functional characterization of distinct critically important bone morphogenetic protein-specific response elements in the Id1 promoter. J Biol Chem 277:4883–4891.

47. Lagna G, A Hata, A Hemmati-Brivanlou and J Massague. (1996). Partnership between DPC4 and SMAD proteins in TGF-beta signalling pathways. Nature 383:832–836.

48. Na K, SW Kim, BK Sun, DG Woo, HN Yang, HM Chung and KH Park. (2007). Osteogenic differentiation of rabbit mesenchymal stem cells in thermo-reversible hydrogel constructs containing hydroxyapatite and bone morphogenic protein-2 (BMP-2). Biomaterials 28:2631–2637.

49. Carvalho RS, JL Schaffer and LC Gerstenfeld. (1998). Osteoblasts induce osteopontin expression in response to attachment on fibronectin: demonstration of a common role for integrin receptors in the signal transduction processes of cell attachment and mechanical stimulation. J Cell Biochem 70:376–390.

50. Roskelley CD, PY Desprez and MJ Bissell. (1994). Extracellular matrix-dependent tissue-specific gene expression in mammary epithelial cells requires both physical and biochemical signal transduction. Proc Natl Acad Sci U S A 91:12378–12382.

51. Connelly JT, JE Gautrot, B Trappmann, DW Tan, G Donati, WT Huck and FM Watt. (2010). Actin and serum response

factor transducer physical cues from the microenvironment to regulate epidermal stem cell fate decision. Nat Cell Biol 12:711–718.

52. Watt FM, PW Jordan and CH O'Neill. (1988). Cell shape controls terminal differentiation of human epidermal keratinocytes. Proc Natl Acad Sci U S A 85:5576–5580.

53. Kallai I, GH van Lenthe, D Ruffoni, Y Zilberman, R Müller, G Pelled, D Gazit. (2010). Quantitative, structural, and image-based mechanical analysis of nonunion fracture repaired by genetically engineered mesenchymal stem cells. J Biomech 43:2315–2320.

54. Thomas CH, JH Collie, CS Sfeir and KE Healy. (2002). Engineering gene expression and protein synthesis by modulation of nuclear shape. Proc Natl Acad Sci U S A 99: 1972–1977.

55. Kelly DJ and CR Jacobs. (2010). The role of mechanical signals in regulating chondrogenesis and osteogenesis of mesenchymal stem cells. Birth Defects Res C Embryo Today 90:75–85.

56. Yoshikawa H, K Yoshioka, T Nakase and K Itoh. (2009). Stimulation of ectopic bone formation in response to BMP-2 by Rho kinase inhibitor: a pilot study. Clin Orthop Relat Res 467:3087–3095.

57. Woods A, G Wang and F Beier. (2005). RhoA/ROCK signaling regulates Sox9 expression and actin organization during chondrogenesis. J Biol Chem 280:1626–1634.

58. Wrana JL. (2000). Crossing Smads. Sci STKE 2000, RE1.

59. Noth U, R Tuli, R Seghatoleslami, M Howard, A Shah, DJ Hall, NJ Hickok and RS Tuan. (2003). Activation of p38 and Smads mediates BMP-2 effects on human trabecular bone-derived osteoblasts. Exp Cell Res 291:201–211.

60. Lee-Hoeflich ST, CG Causing, M Podkowa, X Zhao, JL Wrana and L Attisano. (2004). Activation of LIMK1 by binding to the BMP receptor, BMPRII, regulates BMP-dependent dendritogenesis. EMBO J 23:4792–4801.

61. Theriault BL, TG Shepherd, ML Mujoomdar and MW Nachtigal. (2007). BMP4 induces EMT and Rho GTPase activation in human ovarian cancer cells. Carcinogenesis 28:1153–1162.

62. Batut J, M Howell and CS Hill. (2007). Kinesin-mediated transport of Smad2 is required for signaling in response to TGF-beta ligands. Dev Cell 12:261–274.

63. Edlund S, M Landström, CH Heldin and P Aspenström. (2002). Transforming growth factor-beta-induced mobilization of actin cytoskeleton requires signaling by small GTPases Cdc42 and RhoA. Mol Biol Cell 13:902–914.

64. Dong C, Z Li, R Alvarez, Jr., XH Feng and PJ Goldschmidt-Clermont. (2000). Microtubule binding to Smads may regulate TGF beta activity. Mol Cell 5:27–34.

65. Fukata M, M Nakagawa and K Kaibuchi. (2003). Roles of Rho-family GTPases in cell polarisation and directional migration. Curr Opin Cell Biol 15:590–597.

66. Slack BE and MS Siniaia. (2005). Adhesion-dependent redistribution of MAP kinase and MEK promotes muscarinic receptor-mediated signaling to the nucleus. J Cell Biochem 95:366–378.

67. Saito T, CY Sasaki, LJ Rezanka, P Ghosh and DL Longo. (2010). P52-independent nuclear translocation of RelB promotes LPS-induced attachment. Biochem Biophys Res Comm 391:235–241.

Address correspondence to:
Dr. Christopher S. Chen
Skirkanich Professor of Innovation
Department of Bioengineering
University of Pennsylvania
510 Skirkanich Hall, 210 South 33rd Street
Philadelphia, PA 19104

E-mail: chrischen@seas.upenn.edu

This article has been cited by:

1. Huanhuan Liu, Hongju Peng, Yan Wu, Can Zhang, Youzhi Cai, Guowei Xu, Qin Li, Xiao Chen, Junfeng Ji, Yanzhong Zhang, Hong Wei OuYang. 2013. The promotion of bone regeneration by nanofibrous hydroxyapatite/chitosan scaffolds by effects on integrin-BMP/Smad signaling pathway in BMSCs. *Biomaterials* **34**:18, 4404-4417. [CrossRef]

2. Yu-Sheng Hsiao, Chiung-Wen Kuo, Peilin Chen. 2013. Multifunctional Graphene-PEDOT Microelectrodes for On-Chip Manipulation of Human Mesenchymal Stem Cells. *Advanced Functional Materials* n/a-n/a. [CrossRef]

3. S.-h. Hsu, S. Huang, Y.-C. Wang, Y.-C. Kuo. 2013. Novel nanostructured biodegradable polymer matrices fabricated by phase separation techniques for tissue regeneration. *Acta Biomaterialia* . [CrossRef]

4. Ben P Hung, Daphne L Hutton, Warren L Grayson. 2013. Mechanical control of tissue-engineered bone. *Stem Cell Research & Therapy* **4**:1, 10. [CrossRef]

5. Hongju Peng, Zi Yin, Huanhuan Liu, Xiao Chen, Bei Feng, Huihua Yuan, Bo Su, Hongwei Ouyang, Yanzhong Zhang. 2012. Electrospun biomimetic scaffold of hydroxyapatite/chitosan supports enhanced osteogenic differentiation of mMSCs. *Nanotechnology* **23**:48, 485102. [CrossRef]

6. Gregory H. Underhill. 2012. Stem cell bioengineering at the interface of systems-based models and high-throughput platforms. *Wiley Interdisciplinary Reviews: Systems Biology and Medicine* **4**:6, 525-545. [CrossRef]

7. Giancarlo Forte, Stefania Pagliari, Mitsuhiro Ebara, Koichiro Uto, Janice Kal Van Tam, Sara Romanazzo, Carmen Escobedo-Lucea, Elena Romano, Paolo Di Nardo, Enrico Traversa, Takao Aoyagi. 2012. Substrate Stiffness Modulates Gene Expression and Phenotype in Neonatal Cardiomyocytes In Vitro. *Tissue Engineering Part A* **18**:17-18, 1837-1848. [Abstract] [Full Text HTML] [Full Text PDF] [Full Text PDF with Links] [Supplemental Material]

8. Xiang Yu, Daniel M. Cohen, Christopher S. Chen. 2012. miR-125b Is an Adhesion-Regulated microRNA that Protects Mesenchymal Stem Cells from Anoikis. *STEM CELLS* **30**:5, 956-964. [CrossRef]

9. Ana M.C. Barradas, Hugo A.M. Fernandes, Nathalie Groen, Yoke Chin Chai, Jan Schrooten, Jeroen van de Peppel, Johannes P.T.M. van Leeuwen, Clemens A. van Blitterswijk, Jan de Boer. 2012. A calcium-induced signaling cascade leading to osteogenic differentiation of human bone marrow-derived mesenchymal stromal cells. *Biomaterials* **33**:11, 3205-3215. [CrossRef]

10. Priya R. Baraniak, Marissa T. Cooke, Rabbia Saeed, Melissa A. Kinney, Krista M. Fridley, Todd C. McDevitt. 2012. Stiffening of human mesenchymal stem cell spheroid microenvironments induced by incorporation of gelatin microparticles. *Journal of the Mechanical Behavior of Biomedical Materials* . [CrossRef]

11. Evelyn KF Yim, Michael P Sheetz. 2012. Force-dependent cell signaling in stem cell differentiation. *Stem Cell Research & Therapy* **3**:5, 41. [CrossRef]